

# Investigation of the morphology of the features generated via femtosecond lasers in the interior of a bovine cornea sections

Sinisa Vukelic  
Bucknell University  
Mechanical Engineering Department  
Lewisburg, PA 17837

Panjawat Kongsuwan, Y. Lawrence Yao  
Columbia University  
Mechanical Engineering Department  
New York, NY 10027

## ABSTRACT

Nonlinear absorption of femtosecond laser pulses enables the induction of bubble cavities in the interior of eye cornea without affecting other parts of an eye, a phenomena utilized for flap formation in laser assisted corneal surgery. In the present study laser pulses were focused in the interior of the sections of bovine cornea. Tight focus of the laser pulses results in the plasma formation followed by its explosive expansion, which drives cavity formation. The morphology of the generated features as well as the nature of the physical mechanisms of the phenomenon as a function of process parameters is discussed. Numerical model is proposed to develop predictive capabilities for the feature size and shape and the results are compared against the experimental findings.

## KEYWORDS

Femtosecond Laser, Cornea, Laser Processing,

## 1. INTRODUCTION

Corneal surgery is usually performed to correct refractive errors. In case of Laser in situ keratomileusis (LASIK) this is a two-step process<sup>1</sup>. First, femtosecond laser pulses are deposited into the interior of corneal tissue to form a flap separation. Optical breakdown occurs at the focal point causing vaporization of small volume of a tissue within the stromal lamellae and generating gas cavitation bubbles consisting of carbon dioxide and water. A series of pulses are deposited in controlled manner to create a flap. Flap is then manually removed and excimer laser is utilized to reshape geometry of deeper corneal tissue layers, which have limited regenerative capacity (Figure 1). Another laser-based technique is photorefractive keratectomy (PRK). This is a procedure in which outer and layer of cornea (epithelium) is removed and then laser is used to ablate a small amount of corneal stroma to correct refractive errors and improve vision. In recent times use of femtosecond laser as a potential replacement has been under investigation<sup>2</sup>. PRK does not include creation of permanent flap formation making the ablation easier and eliminate risk of dislocated corneal flaps. On the other side, the procedure may induce more pain and slower recovery.

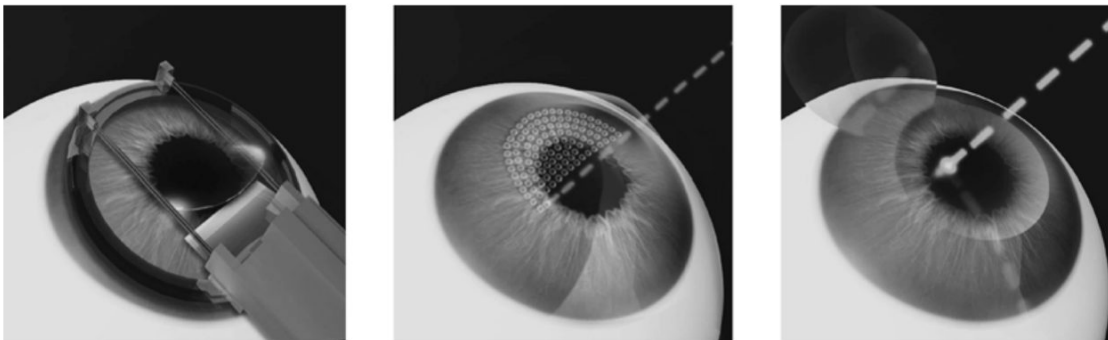


**Figure 1:** The principle of LASIK surgery. During LASIK a thin flap is created by a microkeratome (left). In contrast to common LASIK procedure, the flap is prepared using a laser by fs\_LASIK (middle). Then a remodeling of the cornea underneath the flap with the excimer laser is performed, and the flap is repositioned, finally (right) [37].

Dr. Juhasz and coworkers have done initial studies on use of femtosecond lasers in laser assisted corneal surgery in mid 1990s. Juhasz et al.<sup>3</sup> used water to model shock wave generation and subsequent cavity formation and applied the same method to bovine corneas. Further, it has been shown that femtosecond generated flaps have numerous advantages in comparison to mechanical keratomes including decreased risk of infection and reduced intraocular pressure during the procedure, greater precision and more uniform thickness<sup>4,5</sup>. Lubatschowski<sup>6</sup> has investigated difference in laser-tissue interaction and beam delivery of different commercial systems tailored for refractive surgery. Repetition rate effects on affected tissue have also been studied<sup>7</sup>. Significant differences in the nature of the cell death as function of the laser repetition rate have been observed. At lower repetition rates the laser pulse energy required to create a cut is higher resulting in predominant cell death by necrosis rather than apoptosis. As necrosis causes release of intracellular contents into the surrounding tissue, there is more inflammatory cell influx after flap formation<sup>8</sup>.

Recently some researchers have contemplated use of only fs lasers for the procedure<sup>9</sup>, a topic that has been controversial in past<sup>10,11</sup>. Non-linear nature of the fs laser absorption in transparent dielectrics allows modification of deep corneal layer without removal of the epithelium. This has potential to significantly simplify the surgical procedure, reduce risk of complications and recovery time. However, the mechanics of the bubble formation as well as means to control it is yet to be developed. Further, characterization of the zone affected by the laser-tissue interaction has not been well understood from the engineering point of view.

It is yet to be determined how to control formation of bubbles generated by femtosecond laser pulses. The relationship between laser and parameters determining delivery of the pulse onto the target material is not understood and yet it likely plays significant role in bubble formation. Study presented here addresses fundamental aspects of femtosecond laser interaction with corneal tissue. In addition, to our knowledge, use of high numerical aperture objective lenses to focus ultrafast laser in the interior of a bovine cornea has been utilized for the first time.

## 2. MECHANISM OF FEMTOSECOND LASER PROCESSING OF TRANSPARENT MATERIALS

When an ultrafast laser is focused in the interior of a transparent dielectric, such as fused silica or corneal tissue, due to the ultra-short pulse duration in the order of 10s to 100s of femtoseconds (fs), the intensity in the focal volume rises extremely high ( $>10^{14}$  W/cm<sup>2</sup>) causing *non-linear* energy absorption (Figure 2). The process is independent of the laser wavelength.

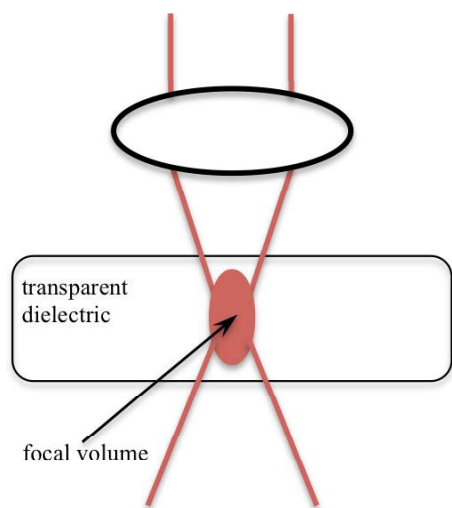


**Figure 2:** Schematic diagram of non-linear absorption mechanisms in laser – transparent dielectric interaction (including cornea); Intensity of the laser beam is intense enough to produce permanent changes in target material only within close proximity of the focal volume.

This unique property enables the interior of the transparent dielectrics to be modified without affecting its surface, where the intensity is not high enough to induce the non-linear effect. The absorption could lead to changes in optical properties, void formation or structural transformation of target material due to thermal accumulation.

Ultrafast lasers have been utilized in non-medical applications such as manufacture of photonic devices; single-step channeling or transmission welding<sup>12</sup>. The mechanism of feature formation in those applications is well understood. Recent applications in corneal surgery showed a lot of promise and commercially available systems appeared on the market in past few years. However, most of research effort has been devoted to parametric studies and characterization of the tissue after the treatment. Fundamental study is needed to fully understand femtosecond-laser tissue interaction and its consequences on surrounding tissue.

It has been well established that the non-linear absorption is triggered by photo-ionization<sup>13</sup> and occurs on a time scale that is much shorter than that for energy transfer from electrons to the lattice. This is due to the heating rate of the electrons in the conduction gap is faster than their cool down by phonon emission. As a result they get free of the valence. Subsequent avalanche ionization<sup>14</sup> enhances growth of free electron density resulting in formation of plasma. High-density, opaque plasma strongly absorbs laser energy through free carrier absorption. Depending on optical and laser processing parameters, the target material

modification can be induced either through *confined microexplosion* or *thermal accumulation*<sup>15</sup>. The former is utilized for flap formation in corneal surgeries whereas latter could be utilized in reshaping of geometry of the endothelium for correction of refractive errors.

If a single pulse is *tightly* focused using high numerical aperture optics into the volume inside of a brittle transparent material, explosive plasma expansion occurs creating a *microexplosion*<sup>16,17</sup>. Energy transfer to ions is done over a few picoseconds, building up very high pressure (~TPa) within the focal volume and causing hydrodynamic motion to commence. Shock wave emerges from the focal volume, compressing the surrounding material. Simultaneously, behind the shock front rarefaction wave propagates into the opposite direction creating a void.

### 2.1. Laser-tissue interaction

Use of femtosecond laser assisted flap formation instead of mechanical microkeratomes yields more uniform flap thickness<sup>8</sup> across the flap diameter, and increased flexibility in terms of flap geometry. Further, occurrence of flap imperfections such as buttonhole flaps is decreased, intraocular pressure is reduced and risk of infection is smaller than when mechanical microkeratomes are utilized<sup>18</sup>. Reduction of clinically significant epithelial growth is also observed<sup>19,20</sup>.

Another major consideration in flap formation is damage induced to the surrounding tissue. This is evaluated through histopathological analysis of corneas after the surgery. Researchers have focused on the type of cell death after the procedure<sup>7</sup>. Two cases are possible, apoptosis and necrosis. Apoptosis is an organized form of cell death in which intracellular components are retained within the apoptotic bodies, a membrane structure that prevents spill of the components into surrounding tissue. On the other hand necrosis is explosive disruption of a cell in which intercellular components are released into surrounding tissue causing its damage. The damage attracts more inflammatory cells to the affected region, which is highly undesirable. Parametric studies have found correlation between the laser repetition rate and apoptosis to necrosis ratio, which suggest that treatment using lasers with higher repetition rates at cause, less damage to the corneal tissue. Simultaneously, it has been shown that use of typical laser pulse energies of 0.8 – 1.2 uJ at high repetition rates (60 kHz) for flap formation produces inflammation levels similar to that of microkeratome<sup>7</sup>. It has further been shown that increase of the laser pulse energy results in increase of necrosis level.

Lubatschowski<sup>6</sup> has suggested that corneal cutting mechanism occurs through action of mechanical forces generated via expansion of cavities that disrupt the tissue. It is assumed that larger forces are generated with higher energy levels, and that the actual cutting occurs at the focal point. However, the exact mechanism is not well understood. Fundamental research is needed to address this issue.

### 3. EXPERIMENTAL SETUP

Fresh bovine eyeballs were obtained from abattoir and corneal discs excised from the eyes within 3 hours from death. Half of the corneas are treated immediately and half were snap frozen with liquid nitrogen and stored in freezer. Frozen corneas were subsequently

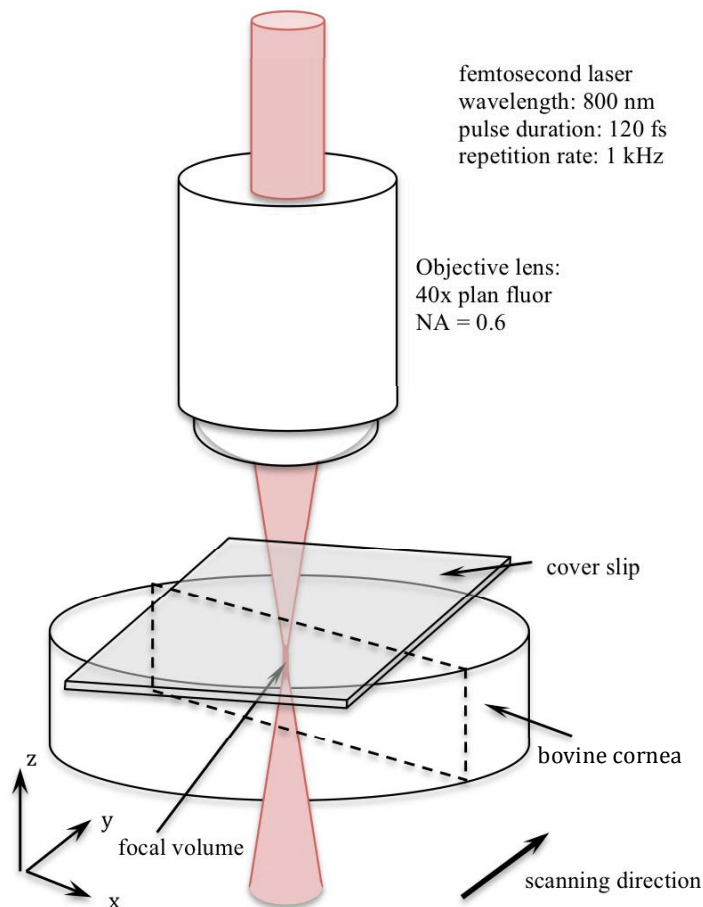


**Figure 3:** Schematic illustration of experimental setup. Laser is focused in the interior of a bovine cornea. cover slip is placed on the top of the bovine cornea specimen to ensure proper focusing conditions. Scanning direction is along y-axis.

thawed and processed with femtosecond laser. No significant difference in experimental results between freshly treated and previously frozen tissue has been observed.

An amplified Ti-Sapphire laser system (Spectra-Physics Hurricane) with pulse duration of 120 fs at 1 kHz repetition rate and 800 nm wavelength was used to conduct experiments. A Zeiss Plan Neofluar 40x objective lens with a NA of 0.6 was employed to focus the laser, providing approximately a 1.5  $\mu\text{m}$  spot size. The beam was focused into the interior of a 4 mm thick, bovine cornea specimen mounted on an Aerotech motorized linear stage to create localized structural changes. A cover slip was placed on top of the sample to prevent scattering of the laser beam at the surface of the sample and thus ensure proper focusing conditions. A schematic diagram of the experimental setup can be seen in Figure 3. A number of different conditions were applied by varying the feedrate of the stage and the energy of the laser pulses. Pulses were applied at energies ranging from 10  $\mu\text{J}$  to 50  $\mu\text{J}$  and stage velocities varied from 0.01 mm/s to 50 mm/s. Generated features were examined with stereographic microscope and transmission optical microscope. Optical micrographs were obtained utilizing diffraction interference contrast (DIC). Both, top and side views were imaged.

## 4. RESULTS AND DISCUSSION

### 4.1. Modeling of the absorption volume

Kongsuwan et al.<sup>21</sup> have developed a model of the spatial distribution of the absorption volume of the femtosecond laser pulse energy deposited in the interior of a transparent material. The model provides insight of the theoretical size of the affected volume within the target material treated by ultrafast lasers. The model is briefly summarized below.

Both, temporal laser intensity profile and temporal distribution of the power of a femtosecond laser pulse tightly focused in the interior of a transparent dielectric follow Gaussian distribution:

$$I(x, y, t) = \frac{2P(t)}{\pi R_o^2} \exp\left(\frac{-2r^2}{R_o^2}\right) \quad (1)$$

$$P(t) = \frac{E_p}{t_p} \sqrt{\frac{4 \ln 2}{\pi}} \exp\left(-4 \ln 2 \left(\frac{t-t_p}{t_p}\right)^2\right) \quad (2)$$

where  $R_o$  is the radius of an unfocused laser beam,  $E_p$  is the laser pulse energy,  $t_p$  is full-width-at-half-maximum (FWHM) of the temporal pulse distribution,  $r$  is the radial distance from the center of laser beam, and  $t$  is time. As a result of such distribution the leading edge of the laser pulse initiates optical breakdown on of the target material at or above the focal plane of the focusing objective, assuming that the laser intensity is larger than the threshold need for breakdown of the target material. Shape of the absorption volume is defined by subsequent temporal slices of the laser pulse, which have higher intensity than the initial ones. The slices produce breakdown upward where the laser beam diameter is larger, which results in teardrop-shaped absorption volume. The top part of the absorption volume has shape of the ellipsoid, and the bottom part can be approximated by a conical frustum. The absorption volume is characterized by volume  $V_{abs}$ , surface area  $S_{abs}$ , longitudinal ( $w_z$ ) and lateral ( $w_{xy}$ ) radii<sup>21</sup>:S

$$V_{abs} = 0.5 \times \frac{4}{3} w_{xy}^2 w_z + \frac{\pi w_z}{3} (w_{xy}^2 + w_{xy} w_o + w_o^2) \quad (3)$$

$$S_{abs} \cong 4\pi (w_{xy}^{2p} + 2w_{xy}^p w_z^p)^{\frac{1}{p}} + \pi (w_{xy} + w_o) \sqrt{(w_{xy} - w_o)^2 + w_z^2} \quad (4)$$

$$w_{xy} = \sqrt{\frac{2P_o}{\pi I_{th} e^2}}; \quad w_z = \frac{\pi w_o^2}{2M^2 \lambda} \sqrt{\frac{2P_o}{I_{th} \pi w_o^2} - 1} \quad (5)$$

where  $w_o$  is diffraction-limited lateral radius, which is a function of the objective numerical aperture (NA) and laser wavelength  $\lambda$ ,  $p$  is a constant,  $P_o$  is the peak power of a laser pulse,  $I_{th}$  is the material intensity threshold,  $M^2$  determines laser beam quality factor.

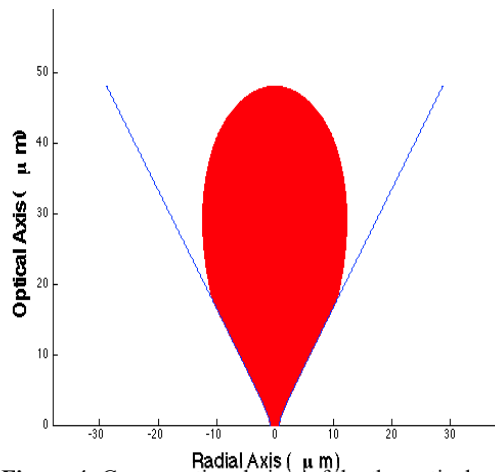


**Figure 4:** Cross-sectional view of the theoretical absorption volume within the target material created by a femtosecond laser pulse with energy 50  $\mu\text{J}$  and focused with objective lens that has  $\text{NA}=0.6$

of about 36 nm<sup>31</sup>. Similarly to other collagen-based tissues, covalent cross-linking stabilizes the molecules. The tissue combines mechanical resilience and optical transparency. These properties are attributed to the nanoscale spatial configuration, consisting of sheets of parallel fibrils<sup>23</sup>. Each sheet is arranged orthogonal to its neighbor and to the light path through cornea. These nanostructures form lamellae, microscale tissue assemblies parallel to the tissue surface at different angles. Such arrangement results in plywood like structure.

Although the type I collagen molecule is rod-like, it contains numerous bends and points of flexibility<sup>24</sup>. Additionally, these structural elements consist of alternating sequences of rigid and flexible domains<sup>25</sup>. Flexible domains are poor in amino acids, proline and hydroxyproline, and are prone to deformation when subject to external forces<sup>26</sup>. Such conformation results in viscoelastic response of collagen fibrils. Elastic behavior corresponds to stretching of collagen triple helices found in cross-linked collagen fibrils, whereas viscous loss involves sliding of collagen fibrils and fibers by each other during tissue deformation<sup>27</sup>.

Viscoelastic material properties and lamellae structure of cornea results in distinctively different femtosecond (fs) laser induced feature formation mechanism than one seen in inorganic transparent dielectrics, used for modeling of laser-tissue interaction<sup>28</sup>. Most inorganic transparent dielectrics processed by fs lasers, such as fused silica or sapphire are brittle. A single tightly focused laser pulse deposited into the interior of a fused silica<sup>12</sup> or sapphire<sup>29</sup> results in plasma formation that expands explosively creating a void. On the other hand, a single femtosecond laser pulse deposited into the interior of corneal tissue creates permanent damage, but not bubbles, as seen in Figure 5. Features depicted are generated with a laser pulses focused about 250  $\mu\text{m}$  below the top surface of a bovine cornea. As seen in the figure, laser affected region is about 15  $\mu\text{m}$  in diameter and thus only one or two lamellae are affected by the laser pulse. The features have distinctively different refractive index from the surrounding tissue

Figure 4 depicts cross-section of the absorption volume generated by a laser pulse with energy of 50  $\mu\text{J}$ , focused with the objective with  $\text{NA} = 0.6$ . The shape of the absorption volume resembles reversed teardrop shape. Feature size is function of the laser pulse energy with higher pulse energies corresponding to larger affected volumes, whereas  $\text{NA}$  determines the shape of the volume. Higher  $\text{NA}$  results in tighter focusing which reduces aspect ratio between longitudinal and lateral radii  $w_z/w_{xy}$ <sup>12</sup>, resulting in more circular shaped features.

#### 4.2. Response of a corneal tissue to femtosecond laser irradiation

Most of collagen can be found in fibrillar form, creating long cylindrical structures. Unlike other macromolecules, collagen fibrils are characterized by axial periodicity and hierarchical structure yielding in macromolecules that provide scaffolding in a form of extracellular matrix. Cornea is a highly specialized tissue that mainly consists of collagen type I molecules co-assembled with type V collagen and forming uniform fibrils with diameter

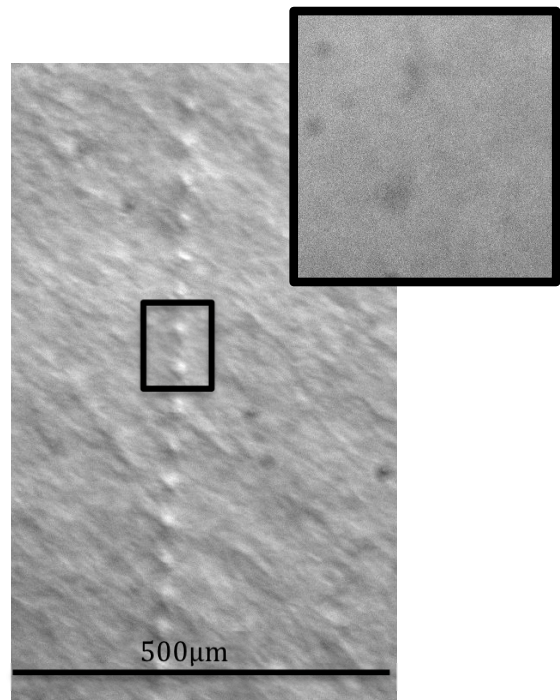


**Figure 5:** Stereographic micrograph of the features generated in the interior of a bovine cornea with individual laser pulses. Top view is presented in the figure. Laser pulse energy is 50  $\mu\text{J}$

suggesting increase of the mismatch between the refractive indices of the collagen fibrils and material in-between within the region affected by the laser pulse<sup>30</sup>.

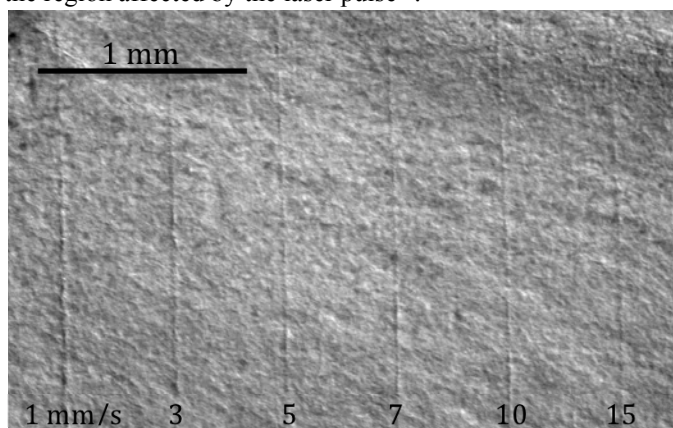


**Figure 6:** Stereographic micrograph of the top view of the features generated with partially overlapping femtosecond laser pulses. Laser pulse energy is kept constant at 30  $\mu\text{J}$  and the feedrate is varied from 1 mm/s to 15 mm/s

Figure 6 shows stereographic image of the top surface of the features generated with trains of femtosecond laser pulses applied to the interior of a bovine cornea. Degree of overlapping of the laser pulses and corresponding affected regions was varied through controlling the stage feedrate. In the figure 6 it can be seen that line like features are formed. The right most line corresponds to feedrate of 15 mm/s at which adjacent affected regions barely touch each other. The laser pulse overlapping increases with decrease of the stage feedrate. With the increase of the percentage of the pulse overlapping, the laser-induced features become more pronounced. It is assumed that the mechanism responsible for the feature formation remains the same as in the previous case when a single pulse is placed into the interior of the target material. Response of cornea to external forces is viscoelastic in part because it serves as buffering mechanism for

volumetric changes in eye, which protects the eye from changes in intraocular pressure<sup>32</sup>. Collagen fibrils in cornea are narrower than in most connective tissues, resulting in larger surface area contact of fibrils with interfibrillar matrix. This likely imparts resistance to plastic deformation. Due to viscoelastic response of the cornea, most of deposited energy is dissipated and, due to small strains, there may be a straightening of the collagen fibrils<sup>33</sup>, but a tissue rupture is absent. With a further decrease of the feedrate, a significant pulse accumulation occurs leading to higher strains, which yields increase of tissue stiffness. In this phase, there may be molecular gliding within the fibrils and ultimately disruption of the fibril structure<sup>34</sup>. Disruption of fibrils leads to tissue rupture likely initiated by a shock wave formation propagating from the focal volume. While the shock wave propagates outside of the focal volume, a rarefaction wave forms and propagates in the opposite direction creating a void, subsequently filled with gaseous products of the laser-matter interaction. Figure 7 depicts diffraction Interference Contrast (DIC) optical micrograph of a gaseous bubble generated in the interior of a bovine cornea specimen, where fig. 7a represents to the top view of the bubbles and 7b corresponds to the side view.

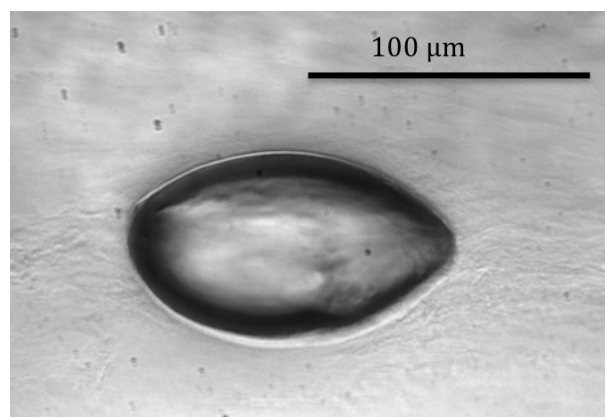
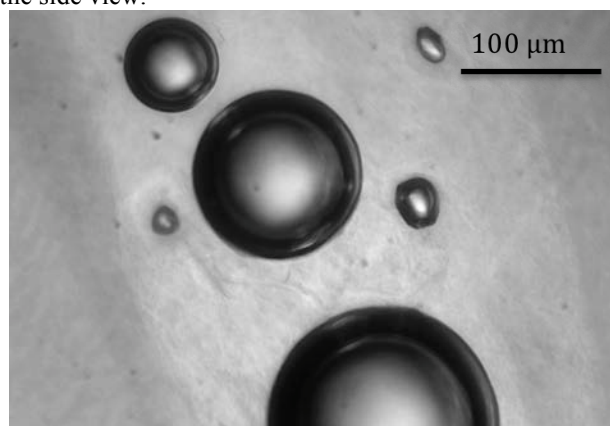


**Figure 7:** Diffraction Interference Contrast (DIC) optical micrograph of a bubble generated in the interior of a bovine cornea by a femtosecond laser (a) top view (b) side view

The bubbles were generated with laser pulse train with energy of 50  $\mu\text{J}$  per pulse at stage feedrate of 0.1 mm/s. The bubbles appear within the laser-affected region, which brighter than surrounding tissue, again due to refractive index change mentioned in the previous paragraph. A dark ring encircling bright interior characterizes the features. Bright region likely correspond to a gas trapped inside of a bubble. Average diameter of the bubbles is about 100  $\mu\text{m}$ , and non-

uniformity in size is attributed to the material heterogeneity. The side view shows that a bubble is slanted, and does not correspond to the shape of absorption volume seen in figure 4. This can be explained by the lamellar structure of a bovine cornea. Propagation of the plasma-initiated shock waves is likely possible in lateral direction along the lamellae, whereas adjacent layers impede deformation propagation in longitudinal direction.

Stress-strain measurements on the cornea yield a characteristic J-shaped curve with distinctive toe, heel and linear regions, followed by the failure strain<sup>33,35</sup>. Jue and Maurice<sup>33</sup> assumed that in absence of tension fibril takes sinusoidal form described by  $y_o = a_o \sin \frac{2\pi x}{\lambda}$ , with wavelength of about 14  $\mu\text{m}$ . This is justified by observations of corneal lamellae via electron microscopy. Therefore, it is assumed that application of tension results in straightening of the fibrils, which correspond to an viscoelastic response of the tissue to the external forces. Similar conclusions have been drawn for collagen tissue found in rat-tail tendons<sup>34</sup>. A theoretical model describing tension in corneal tissue is proposed<sup>33</sup>:

$$\sigma = EI \left( \frac{2\pi}{\lambda} \right)^2 \left[ \left( \frac{\epsilon_\infty}{\epsilon_\infty - \epsilon} \right)^{\frac{1}{2}} - 1 \right] \quad (6)$$

where  $\sigma$  is tension in fibril,  $E$  is the Young's modulus of collagen,  $I$  is fibril cross-sectional moment of inertia and  $\epsilon$  and  $\epsilon_\infty$  are actual and maximum strains in fibril, respectively. Features created by single laser pulses and relatively modest pulse overlapping may fall into toe and heel regions where deformation is mostly characterized by straightening of the collagen fibrils<sup>33</sup>, and somewhat within the linear region characterized by gliding of the neighboring molecules<sup>34</sup>. Bubble formation likely occurs when the strain reaches certain threshold past the linear region. At that point collagen disruption may be analogous to the instable crack propagation in fracture mechanics. However, due to complex nature of loading due to deposition of the ultrafast laser pulses in the interior of corneal tissue, the analogies drawn are approximate. The future studies will address this matter in considerably more detail.

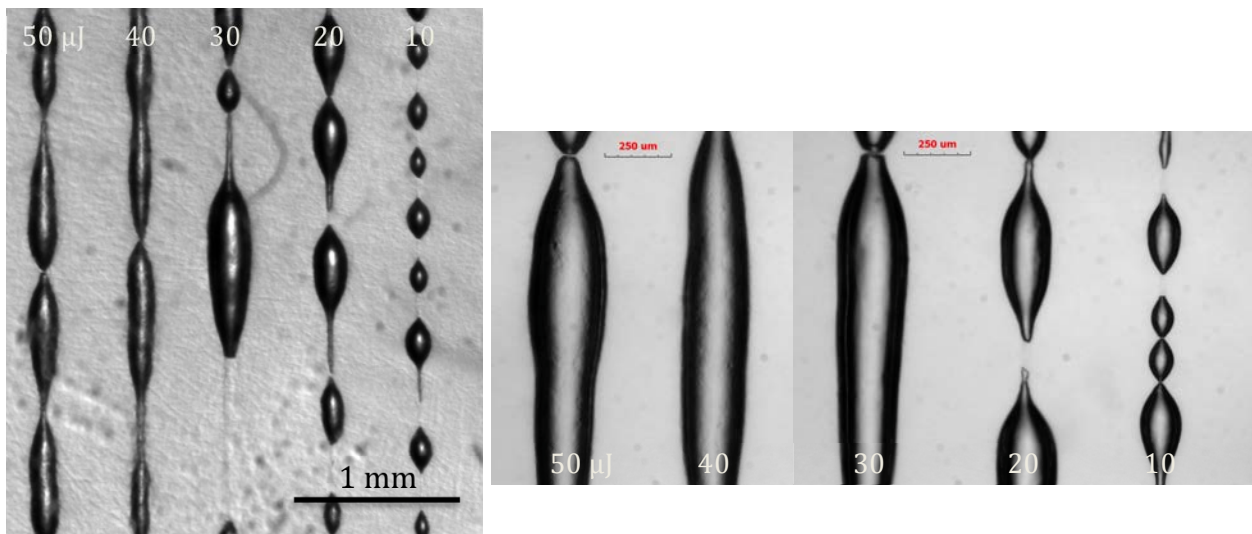


**Figure 8:** the top view of channels generated in the interior of a bovine cornea by a femtosecond laser. Laser pulse energy was varied between 50  $\mu\text{J}$  and 10  $\mu\text{J}$  at constant feedrate of 0.1 mm/s (a) Stereographic micrograph (b) Diffraction Interference Contrast (DIC) optical micrograph of enlarged segment of the features.

### 4.3. Channel Formation

Figure 8 shows channels created in the interior of the bovine cornea made by trains of femtosecond laser pulses with pulse energies ranging from 10  $\mu\text{J}$  to 50  $\mu\text{J}$  at constant stage feedrate of 0.1 mm/s. From the figure it can be seen that laser pulse energy does not influence the size of the diameter of the channels, but rather the continuity of the produced features. Channel produced with the highest laser pulse energy, although showing some periodicity is rather uniform. On the other hand, decrease of the pulse energy, results in less uniform channels. Simultaneously, diameter of the produced

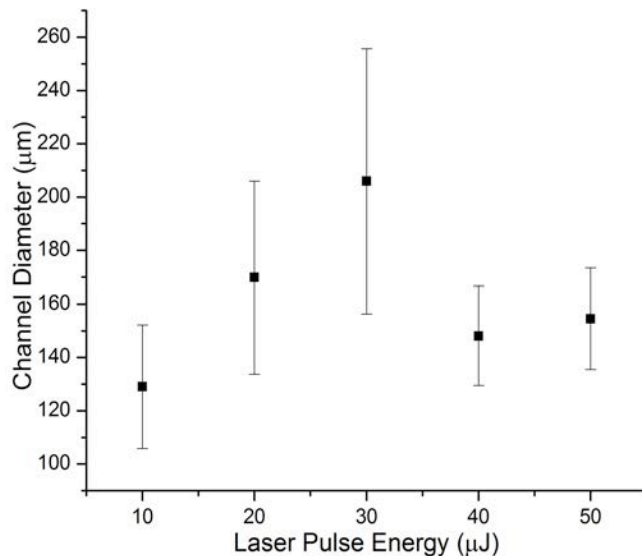


**Figure 9:** Variation of the channel diameter as a function of laser pulse energy.

tissue interaction has been investigated and mechanism for tissue response to femtosecond laser treatment proposed. Viscoelastic material properties of bovine cornea result in feature formation mechanism distinctively different from inorganic brittle transparent solids such as fused silica or sapphire. Laser pulse energy and feedrates have been varied to investigate size and shape of feature formation as a function of processing parameters.

#### ACKNOWLEDGEMENT

The authors would like to express deepest gratitude to Dr. Matthew B. Heintzelman, Associate Professor in the Biology department at Bucknell University for useful suggestions and help with sample preparation.

#### REFERENCES:

- [1] Soong, H. K., Malta, J. M., "Femtosecond Lasers in Ophthalmology," *American Journal of Ophthalmology* 147(2), 189-197 (2009)
- [2] Vodavalli, P. K., Hurmeric, V., Yoo, S. H., "Air bubble in anterior chamber as indicator of full-thickness incisions in femtosecond-assisted astigmatic keratotomy," *Journal of Cataract and Refractive Surgery*, 37(9), 1723-1725 (2011)
- [3] Juhasz, T., Kastis, G. A., Suarez, C., Bor, Z., Bron, W. E., "Time-Resolved Observations of Shock Waves and Cavitation Bubbles Generated by Femtosecond Laser Pulses in Corneal Tissue and Water," *Lasers in Surgery and Medicine* 19, 23-31 (1996)
- [4] Kezirian G. M., Stonecipher, K. G., "Comparison of the IntraLase femtosecond laser and mechanical keratomes for laser in situ keratomileusis," *Journal of Cataract and Refractive Surgery*, 30(4), 804-811 (2004)
- [5] Davison J. A., Johnson, S. C., "Intraoperative complications of LASIK flaps using the IntraLase femtosecond laser in 3009 cases," *J Refract Surg.* 26(11), 851-857 (2010)
- [6] Lubatschowski, H., "Overview of commercially available femtosecond lasers in refractive surgery," *J Refract Surg.* 24, S102-S107 (2008)
- [7] Netto, M. V., Mohan, R. R., Medeiros, F. W., Dupps, Jr, W. J., Sinha, S., Krueger, R. R., Stapleton, W. M., Rayborn, M., Suto, C., Wilson, S. E., "Femtosecond Laser and Microkeratome Corneal Flaps: Comparison of Stromal Wound Healing and Inflammation," *Journal of Refractive Surgery*, 23, 667-676, (2007)
- [8] Medeiros, F. W., Stapleton, W. M., Hammel, J., Krueger, R. R., Netto, M. V., Wilson, S. E., "Wavefront Analysis Comparison of LASIK Outcomes With the Femtosecond Laser and Mechanical Microkeratomes," *Journal of Refractive Surgery*, 23, 880-887, (2007)
- [9] Meltendorf, C., Deller, T., Ackermann, H., von Pape, U., "Corneal intrastromal tissue modeling with the femtosecond laser," *Graefes Arch Clin Exp Ophthalmol* 249, 1661-1666, (2011)
- [10] Vogel, A., Gunther, T., Asiyo-Vogel, M., Birngruber, R., "Factors determining the refractive effects of intrastromal photorefractive keratectomy with the picosecond laser." *J Cataract Refract Surg.*, 23, 1301-1310, (1997)

channels appears not to be a function of laser pulse energy (Figure 9). This may be explained by the heterogeneity of the tissue in which damage threshold at which bubbles are formed is not a fixed value, but rather a range. Thus, at high pulse energies it is more likely that the threshold within a particular corneal lamellae is reached along the laser path at almost all times, whereas with the decrease of the pulse energy this is not the case. In addition, relatively uniform channel diameter of all produced channels indicates that once the threshold is reached, laser pulses do not drive bubble and channel formation anymore. It should be also noted that features are larger in size if the laser pulses are located closer to the surface, which leads to conclusion that a portion of the laser energy is absorbed during the laser propagation through the tissue.

#### 5. CONCLUSION

Interaction between tightly focused femtosecond laser pulses in the interior of a bovine cornea and the corresponding affected tissue has been studied. Laser-

- [11] Vogel, A., Gunther, T., Asiyovogel, M., Birngruber, R., "Studies of the development of refractive effects in intrastromal refractive corneal surgery with the picosecond laser," *Ophthalmologie* 94, 467–474, (1997)
- [12] Vukelic, S., Kongsuwan, P., Yao, Y. L., (2010) "Ultra-Fast Laser Induced Structural Modification of Fused Silica. Part I: Feature Formation Mechanisms," *Journal of Manufacturing Science and Engineering*, 132, 061012-1, (2010)
- [13] Keldysh, L. V., "Ionization in the Field of a Strong Electromagnetic Wave," *Soviet Physics JETP* 20, 1307-1314, (1967)
- [14] Stuart B.C., Feit, M.D., Rubenchik, A.M., Shore, B.W., Perry, M.D. "Laser Induced Damage in Dielectrics with Nanosecond to Subpicosecond Pulses," *Physical Review Letters* 74, 2248-2251, (1995)
- [15] Schaffer C. B., Garcia, J. F., Mazur, E., "Bulk Heating of Transparent Materials Using a High-Repetition-Rate Femtosecond Laser," *Applied Physics A* 76, 351-354, (2003)
- [16] Sundaram, S. K., Schaffer, C. B., Mazur, E. "Microexplosions in Tellurite Glasses," *Applied Physics A* 76, 379-384, (2003)
- [17] Juodkazis, S., Misawa, H., Hashimoto, T., Gamaly, E. G., Luther-Davies, B. "Laser-Induced Microexplosion Confined in a Bulk of Silica: Formation of Nanovoids," *Applied Physics Letters* 88, 201909-1 - 201909-3, (2006)
- [18] Haft P., Yoo S. H., Kymionis G. D., Ide T., O'Brien T. P., Culbertson W. W., "Complications of LASIK flaps made by the intraLase 15- and 30 kHz femtosecond lasers," *J Refract Surg.*, 25, 979–84, (2009)
- [19] Letko E., Price, M. O., Price, F. W., Jr. "Influence of original flap creation method on incidence of epithelial ingrowth after LASIK retreatment," *J Refract Surg.*, 25(11), 1039-1041, (2009)
- [20] Kamburoglu G., Ertan, A., "Epithelial in growth after femtosecond laser-assisted *in situ* keratomileusis," *Cornea*, 27, 1122–1125, (2008)
- [21] Kongsuwan, P., Satoh, G., Yao, Y.L., "Transmission welding of glass by femtosecond laser: mechanism and fracture strength", *ASME Trans. Journal of Manufacturing Science and Engineering*, 134, 011004-1 - 011004-11, (2012)
- [22] Birk, D. E., Zycband, E. I., Winkelmann, D. A., Trelstad, R. L., "Collagen fibrillogenesis *in situ*: fibril segments are intermediates in matrix assembly," *Proc Natl Acad Sci USA*, 86, 4549–4553, (1989)
- [23] Holmes, D. F., Gilpin, C. J., Baldock, C., Ziese, U., Koster, A. J., Kadler, K. E. "Corneal collagen fibril structure in three dimensions: Structural insights into fibril assembly, mechanical properties, and tissue organization," *PNAS* 98, 7307–7312, (2001)
- [24] Silver, F. H., Birk, D. E., "Molecular structure of collagen in solution: Comparison of types I, II, III, and V," *Int. J. Biol. Macromol.*, 6, 125–132, (1984)
- [25] Landis, W. J., Silver, F. H., Freeman, J., "Collagen as a scaffold for biomimetic mineralization of vertebrate tissues," *J. Mater. Chem.*, 16, 1495–1503, (2006)
- [26] Freeman, J. W., Silver, F. H., "Elastic energy storage in unmineralized and mineralized extra-cellular matrices (ECMs): A comparison between molecular modeling and experimental measurements," *J. Theor. Biol.* 229, 371–381, (2004)
- [27] Silver, F. H., Christiansen, D. L., Snowhill, P. B., Chen, Y., "Transition from viscous to elastic-based dependency of mechanical properties of self-assembled type I collagen fibers," *J. Appl. Polym. Sci.* 79, 134–142, (2001)
- [28] Vartapetov, S. K., Khudyakov, D. V., Lapshin, K. E., Obidin, A. Z., Sheherbakov, I. A., "Femtosecond lasers for microsurgery of cornea," *Quantum Electronics* 42 (3) 262-268, (2012)
- [29] Gamaly, E.G., Juodkazis, S., Nishimura, K., Misawa, H., Luther-Davies, B., Hallo, L., Nicolai, P., Tikhonchuk, V. T. "Laser-Matter Interaction in the Bulk of a Transparent Solid: Confined Microexplosion and Void Formation," *Physical Review B* 73, 214101-1 - 214101-15, (2006)
- [30] Meek, K. M., Leonard, D. W., Connon, C., Dennis, S., Khan, S., Transparency, swelling and scarring in the corneal stroma," *Eye*, 17, 927–936, (2003)
- [31] Chakravarti, S., Magnuson, T., Lass, J. H., Jepsen, K. J., LaMantia, C., Carroll, H., "Lumican Regulates Collagen Fibril Assembly: Skin Fragility and Corneal Opacity in the Absence of Lumican," *The Journal of Cell Biology*, 141(5), 1277–1286, (1998)
- [32] Johnson, C. S., Mian, S. I., Moroi, S., Epstein, D., Izatt, J., Afshari, N. A., "Role of corneal elasticity in damping intraocular pressure," *Invest. Ophthalmol. Vis. Sci.*, 48, 2540–2544, (2007)
- [33] Jue, B., Maurice, D. M., "The mechanical properties of the rabbit and human cornea," *J. Biomech.*, 19, 847–853, (1986)
- [34] Fratzl, P., Misof, K., Zizak, I., Rapp, G., Amenitsch, H., Bernstorff, S., "Fibrillar structure and mechanical properties of collagen," *J. Struct. Biol.* 1122, 119–22, (1998)
- [35] Roeder, B. A., K. Kokini, J. E. Sturgis, J. P. Robinson, and S. L. Voytik-Harbin. "Tensile mechanical properties of three-dimensional type I collagen extracellular matrices with varied microstructure," *J. Biomech. Eng.*, 124, 214–222,

(2002)

[36] Fratzl, P., [Collagen Structure and Mechanics] Springer, New York, 2008

[37] Sander, M., Minet, O., Zabarylo, U., Muller, M., Tetz, M. R., "Comparison of Retina Damage Thresholds Simulating the Femtosecond-Laser in situ Keratomileusis (fs-LASIK) Process with Two Laser Systems in the CW- and fs-Regime," Laser Physics, 22(4), 805-812, (2012)